Exchange effects in electron-impact ionization of atomic hydrogen

H. Ray and A. C. Roy
Department of Physics, University of Kalyani, Kalyani 741235, West Bengal, India
(Received 9 October 1990; revised manuscript received 16 June 1992)

A method for obtaining the exchange scattering amplitude for electron-impact ionization of atomic hydrogen in the eikonal approximation is developed. The expression for the eikonal amplitude in the present case turns out to be a two-dimensional integral which can be evaluated numerically with convenience. This exchange amplitude can be combined with the corresponding direct amplitude to calculate both differential and total cross sections for electron-impact ionization of hydrogen atoms. We present numerical results for triply differential cross sections (TDCS) for the $H(e,2e)H^+$ process for incident energies of 150 and 250 eV. A comparison is made of the present TDCS with the corresponding results of other calculations and experiment.

PACS number(s): 34.80.Dp

I. INTRODUCTION

During the past and the present decade, the eikonal and Glauber approximations have been useful theoretical tools for studying a wide variety of atomic collision processes [1]. In particular, these approximations have been successful in intermediate- and high-energy collision processes.

In 1972 Byron and Joachain [2] first applied the eikonal approximation (EA) to calculate the e^--H exchange amplitude for elastic scattering. They used a straightforward Monte Carlo integration technique to compute the six-dimensional integral occurring in the expression for the amplitude. Later on, Foster and Williamson [3] reduced this integral to a two-dimensional one. However, the numerical evaluation of this integral involves computational difficulties and requires extreme care. Recently, Onaga, Tsuji, and Narumi [4] have developed a useful method for calculating the eikonal exchange amplitude for e^--H scattering without the difficulty related to numerical convergence and found agreement with the exact results of Franco and Halpern [5] and Gien [6]. The method was, however, applied to elastic scattering.

In 1980 Sekimura and Narumi [7] applied the EA to obtain the exchange amplitude for electron-impact ionization for atomic hydrogen. They succeeded in reducing the six-dimensional exchange amplitude to a three-dimensional form. The method, however, was based on a partial-wave decomposition of the scattering amplitude and the final expression for the amplitude involved summations over the orbital angular momentum l and the projection quantum number m of the ejected electron.

This paper reports a calculation of the exchange scattering amplitude in the EA for electron-impact ionization of atomic hydrogen. In order to evaluate the amplitude, we have avoided the use of partial-wave decomposition since these procedures require substantial computer time where many partial waves are involved. Our procedure, which is an extension of the method of Onaga, Tsuji,and Narumi [4], leads to a two-dimensional integral for the exchange amplitude for the H $(e,2e)H^+$ process, which can be computed numerically with convenience. As an illustration of the exchange effects, we calculate triply differential cross sections (TDCS's) [8] by combining this exchange amplitude with the direct amplitude previously obtained by us in the Glauber approximation (GA) [9]. We have also incorporated in the present calculation the effect of post-collision interaction (PCI) using the method of Klar *et al.* [10] and compared our results with the absolute data of Ehrhardt *et al.* [11], who made extensive measurements of TDCS's in the case of asymmetric geometry, where one of the two emitting electrons has a much smaller energy than the other.

The plan of this paper is as follows: Section II gives the theoretical formulation of obtaining the TDCS's for electron-impact ionization of hydrogen. In Sec. II A we describe the reduction of the eikonal exchange amplitude for $H(e,2e)H^+$ reactions to a two-dimensional integral. Section II B gives the method of obtaining TDCS's. In Sec. III we present the results of our numerical calculation of the TDCS's and compare them with the corresponding results of other theoretical calculations and experiment. Section IV contains the conclusions. Atomic units are used throughout unless otherwise indicated.

II. THEORY

A. Exchange amplitude

In this section we derive the exchange scattering amplitude for e^--H ionization in the eikonal approximation. Although the exchange amplitude is considered in both post and prior forms, we consider the post form; however, our procedure can be easily applied to the prior form. Also, we confine our attention to the case of asymmetric geometry, where one of the emitting particles is fast, while the other one is slow.

Let $\mathbf{r}_1$ be the position vector of the incident electron and $\mathbf{r}_2$ the position vector of the electron initially bound to the proton. Let $\mathbf{k}$, $\mathbf{k}_1$, and $\mathbf{k}_2$ denote, respectively, the momenta of the incident, scattered (fast), and ejected (slow) electrons. The exchange-transition matrix element

is given by [12]

$$T_{fi}=\left\langle \Phi_f(2,1)\left|\frac{1}{r_{12}}-\frac{1}{r_2}\right|\psi_i^{(+)}(1,2)\right\rangle , \tag{1}$$

where i and f denote the initial and final states. In Eq. (1), Φ_f is given by

$$\Phi_f(\mathbf{r}_2,\mathbf{r}_1)=e^{i\mathbf{k}_1\cdot\mathbf{r}_2}\phi_f(\mathbf{r}_1) , \tag{2}$$

where $\phi_f(\mathbf{r})$ represents the wave function of the ejected (slow) electron and is taken to be the Coulomb wave function

$$\phi_f(\mathbf{r})=(2\pi)^{-3/2}e^{\gamma\pi/2}\Gamma(1+i\gamma)e^{i\mathbf{k}_2\cdot\mathbf{r}}\,{}_1F_1(-i\gamma,1,-i(k_2r+\mathbf{k}_2\cdot\mathbf{r})) , \tag{3}$$

with $\gamma=1/k_2$, where ${}_1F_1$ is the confluent hypergeometric function.

In the eikonal approximation, the wave function $\psi_i^{(+)}$ is given approximately by

$$\psi_i^{(+)}(\mathbf{r}_1,\mathbf{r}_2)=\phi_i(\mathbf{r}_2)\exp\left[i\mathbf{k}\cdot\mathbf{r}_1-\frac{i}{k}\int_{-\infty}^{z_1}dz_1'\,V_i(\mathbf{b}_1+z_1'\hat{\mathbf{z}},\mathbf{r}_2)\right] , \tag{4}$$

where $\mathbf{r}_1$ has been decomposed into vectors parallel and perpendicular to the path of integration, which is along a vector $\hat{\mathbf{z}}$. In the present case of post interation, $\hat{\mathbf{z}}$ is along the direction of the incident beam $\mathbf{k}$. In Eq. (4), ϕ_i represent the initial state of the target atom and is given by

$$\phi_i(\mathbf{r})=\pi^{-1/2}\exp(-\alpha r) , \tag{5}$$

with $\alpha=1$, and the integral for the eikonal phase is given by

$$\int_{-\infty}^{z_1}V_i(\mathbf{b}_1+z_1'\hat{\mathbf{z}},\mathbf{r}_2)dz_1'=\ln\left[\frac{r_1-\mathbf{r}_1\cdot\hat{\mathbf{z}}}{r_{12}-\mathbf{r}_{12}\cdot\hat{\mathbf{z}}}\right] . \tag{6}$$

Using Eqs. (2), (4), and (6), Eq. (1) can be written as

$$T_{fi}=\int d\mathbf{r}_1d\mathbf{r}_2e^{-i\mathbf{k}_1\cdot\mathbf{r}_2}\phi_f^*(\mathbf{r}_1)\left[\frac{1}{r_{12}}-\frac{1}{r_2}\right]e^{i\mathbf{k}\cdot\mathbf{r}_1}\phi_i(\mathbf{r}_2)\left[\frac{r_{12}-\mathbf{r}_{12}\cdot\hat{\mathbf{z}}}{r_1-\mathbf{r}_1\cdot\hat{\mathbf{z}}}\right]^{i\eta} , \tag{7}$$

where $\eta=1/k$.

We may write the amplitude (7) as a sum of two terms:

$$T_{fi}=t_{fi}[r_{12}]+t_{fi}[r_2] , \tag{8}$$

where $t_{fi}[r_{12}]$ and $t_{fi}[r_2]$ are the terms in Eq. (7) corresponding to the electron-electron and electron-nucleus parts of the interaction potential, respectively.

Let us first consider $t_{fi}[r_{12}]$. From the definition of the Γ function, we have the relation

$$\alpha^{-z}=\frac{1}{\Gamma(z)}\int_0^\infty t^{z-1}e^{-\alpha t}dt , \tag{9}$$

for $\mathrm{Re}(\alpha)>0$, $\mathrm{Re}(z)>0$. Utilizing (9), $t_{fi}[r_{12}]$ can be expressed as

$$t_{fi}(r_{12})=\frac{1}{|\Gamma(i\eta)|^2}t_A , \tag{10}$$

where

$$t_A=\int_0^\infty dt\,t^{i\eta-1}\int_0^\infty ds\,s^{-i\eta-1}\int d\mathbf{r}_1d\mathbf{r}_2\phi_f^*(\mathbf{r}_1)\exp(-i\mathbf{k}_1\cdot\mathbf{r}_2)\exp(-r_1t)\frac{1}{r_{12}}\phi_i(\mathbf{r}_2)\exp\{i(\mathbf{k}-it\hat{\mathbf{z}})\cdot\mathbf{r}_1\}\exp\{-(r_{12}-z_{12})s\} , \tag{11}$$

with $z_{12}=\mathbf{r}_{12}\cdot\hat{\mathbf{z}}$.

Replacing $r_{12}^{-1}\exp[-s(r_{12}-z_{12})]$ by its Fourier transform

$$r_{12}^{-1}\exp[-s(r_{12}-z_{12})]=\frac{1}{2\pi^2}\int d\mathbf{p}\frac{\exp[i\mathbf{p}\cdot(\mathbf{r}_1-\mathbf{r}_2)]}{(\mathbf{p}+is\hat{\mathbf{z}})^2+s^2} \tag{12}$$

and then using Eqs. (3) and (5), we have

$$t_A = c' \int_0^\infty dt\, t^{i\eta-1} \int_0^\infty ds\, s^{-i\eta-1} \int d\mathbf{p} \frac{1}{(\mathbf{p}+is\hat{\mathbf{z}})^2+s^2} \times \int d\mathbf{r}_1 e^{i(\mathbf{q}'-\mathbf{k}_2)\cdot\mathbf{r}_1 - tr_1} {}_1F_1(i\gamma,1,i(k_2 r_1+\mathbf{k}_2\cdot\mathbf{r}_1)) \int d\mathbf{r}_2 e^{-i\mathbf{k}\cdot\mathbf{r}_2-\alpha r_2-i\mathbf{p}\cdot\mathbf{r}_2}, \tag{13}$$

where

$$c' = 2^{-5/2}\pi^{-4} e^{\gamma\pi/2}\Gamma(1-i\gamma)$$

and

$$\mathbf{q}' = \mathbf{p}+\mathbf{k}-it\hat{\mathbf{z}} .$$

We next introduce the following integral representation of the confluent hypergeometric function [13]:

$${}_1F_1(ix,1,\omega) = \frac{1}{2\pi i} \oint_\Gamma dt\, t^{-1+ix}(t-1)^{-ix} e^{\omega t}, \tag{14}$$

where Γ indicates a closed contour encircling each of the two points 0 and 1 once counterclockwise. On using Eq. (14) in Eq. (13) and performing integrations over $\mathbf{r}_1$ and $\mathbf{r}_2$, we get

$$t_A = -32i\pi\alpha c' \oint_\Gamma dt_1 t_1^{-1+i\gamma}(t_1-1)^{-i\gamma} \int_0^\infty dt\, t^{i\eta-1} t' \int_0^\infty ds\, s^{-i\eta-1} \times \int d\mathbf{p} \frac{1}{(\mathbf{p}+is\hat{\mathbf{z}})^2+s^2} \frac{1}{[(\mathbf{q}''-\mathbf{k}_2)^2+t'^2][(\mathbf{k}_1+\mathbf{p})^2+\alpha^2]^2}, \tag{15}$$

where

$$\mathbf{q}'' = \mathbf{p}+\mathbf{k}+t_1\mathbf{k}_2-it\hat{\mathbf{z}}$$

and

$$t' = t - ik_2 t_1 .$$

We express Eq. (15) as

$$t_A = -8i\pi c' \oint_\Gamma dt_1 t_1^{-1+i\gamma}(t_1-1)^{-i\gamma} \int_0^\infty dt\, t^{i\eta-1} \int_0^\infty ds\, s^{-i\eta-1} \frac{\partial}{\partial t'} \frac{\partial}{\partial \alpha} \times \int d\mathbf{p} \frac{1}{[(\mathbf{p}+is\hat{\mathbf{z}})^2+s^2][(\mathbf{q}''-\mathbf{k}_2)^2+t'^2][(\mathbf{k}_1+\mathbf{p})^2+\alpha^2]} . \tag{16}$$

Making use of the Feynman identity

$$\int_0^1 \frac{1}{[ax+b(1-x)]^2} dx = \frac{1}{ab}, \tag{17}$$

Eq. (16) can be written as

$$t_A = 8i\pi c' \oint_\Gamma dt_1 t_1^{-1+i\gamma}(t_1-1)^{-i\gamma} \int_0^\infty dt\, t^{i\eta-1} \int_0^\infty ds\, s^{-i\eta-1} \frac{\partial}{\partial t'} \frac{\partial}{\partial \alpha} \int_0^1 dx \frac{\partial}{\partial \rho^2} \int d\mathbf{p} \frac{1}{(\mathbf{p}-\mathbf{Q})^2+\rho^2} \frac{1}{[(\mathbf{p}-it\hat{\mathbf{z}})^2+t'^2]}, \tag{18}$$

where

$$\rho^2 = (\alpha^2+k_1^2)x - [\mathbf{k}_1 x + is\hat{\mathbf{z}}(1-x)]^2 \tag{19}$$

and

$$\mathbf{Q} = \mathbf{k}+\mathbf{k}_2(t_1-1)-\mathbf{k}_1-(x-1)\mathbf{k}_1-is\hat{\mathbf{z}}(1-x) . \tag{20}$$

Using the Feynman's identity (17) again, the $\mathbf{p}$ integral in Eq. (18) can be expressed as

$$\int d\mathbf{p} \frac{1}{(\mathbf{p}-\mathbf{Q})^2+\rho^2} \frac{1}{[(\mathbf{p}-it\hat{\mathbf{z}})^2+t'^2]} = \int_0^1 dy \int d\mathbf{p} \frac{1}{(\mathbf{p}^2+\Delta)^2}, \tag{21}$$

where

$$\Delta = (i\mathbf{Q}+\hat{\mathbf{z}}t)^2 y^2 + [\rho^2 - (i\mathbf{Q}+\hat{\mathbf{z}}t)^2 - t'^2]y + t'^2 . \tag{22}$$

The p integral in Eq. (21) can be easily performed. Equation (18) then can be written as

$$t_A = 8i\pi^3 c' \oint_\Gamma dt_1 t_1^{-1+i\gamma}(t_1-1)^{-i\gamma}\int_0^\infty ds\, s^{-i\eta-1}\frac{\partial}{\partial\alpha}\int_0^1 dx\frac{\partial}{\partial\rho^2}M \ , \tag{23}$$

where

$$M = \int_0^\infty dt\, t^{i\eta-1}\frac{\partial}{\partial t'}\int_0^1 dy\frac{1}{\Delta^{1/2}} \ . \tag{24}$$

In order to evaluate the M integral, we first carry out the differentiation with respect to t' and then perform the y and t integrals. Consequently, we have

$$M = -2[(\rho-ik_2t_1)^2+Q^2]^{i\eta-1}[2(\rho-ik_2t_1-iQ_z)]^{-i\eta}\mathcal{B}(i\eta,1-i\eta) \ , \tag{25}$$

where $\mathcal{B}(x,y)$ represents the beta function [14]. Using (25) in (23), we have

$$t_A = -16i\pi^3 c' 2^{-i\eta}\mathcal{B}(i\eta,1-i\eta)\int_0^\infty ds\, s^{-i\eta-1}\int_0^1 dx\frac{\partial}{\partial\alpha}\frac{\partial}{\partial\rho^2}T \ , \tag{26}$$

where

$$T = \oint_\Gamma dt_1 t_1^{-1+i\gamma}(t_1-1)^{-i\gamma}(\rho-ik_2t_1-iQ_z)^{-i\eta}[(\rho-ik_2t_1)^2+Q^2]^{i\eta-1} \ . \tag{27}$$

The T integral can be performed utilizing the result

$$I = \oint_\Gamma dt\, t^{-1+i\alpha}(t-1)^{-i\alpha}(t+\mu)^{-i\eta}(t+\nu)^{i\eta-1}$$
$$= 2\pi i\mu^{-i\eta}\nu^{i\eta-1}\left[1+\frac{1}{\nu}\right]^{-i\alpha}{}_2F_1\left[i\alpha;i\eta;1;\frac{\mu-\nu}{\mu(\nu+1)}\right] . \tag{28}$$

A derivation of the aforesaid result is given in the Appendix. Equation (26) then becomes

$$t_A = 32\pi^4 c' 2^{-i\eta}\mathcal{B}(i\eta,1-i\eta)\int_0^\infty ds\, s^{-i\eta-1}\int_0^\infty dx\frac{\partial}{\partial\alpha}\frac{\partial}{\partial\rho^2}A^{-i\eta}B^{i\eta-1}\mu^{-i\eta}\nu^{i\eta-1}\left[1+\frac{1}{\nu}\right]^{-i\gamma}{}_2F_1\left[i\gamma;i\eta;1;\frac{\mu-\nu}{\mu(\nu+1)}\right] , \tag{29}$$

where

$$A = -i(k_2+\mathbf{k}_2\cdot\hat{\mathbf{z}}) \ , \tag{30}$$

$$\mu = A^{-1}[\rho+i\{(-\mathbf{k}+\mathbf{k}_1+\mathbf{k}_2)\cdot\hat{\mathbf{z}}+is(1-x)\}] \ , \tag{31}$$

$$B = 2[\mathbf{k}_1\cdot\{\mathbf{k}-\mathbf{k}_1x-is\hat{\mathbf{z}}(1-x)\}-k_2^2-ik_2\rho] \ , \tag{32}$$

and

$$\nu = B^{-1}[(\alpha^2+k_1^2)x+(\mathbf{k}-\mathbf{k}_2)^2-2(\mathbf{k}-\mathbf{k}_2)\cdot\{\mathbf{k}_1x+is\hat{\mathbf{z}}(1-x)\}] \ . \tag{33}$$

Using (29) in (10), we can obtain the contribution of the amplitude corresponding to the electron-electron part of the interaction potential. A similar analysis may be performed to obtain $t_{fi}[r_2]$, i.e., the amplitude due to electron-nucleus part. The results may be combined to yield for T_{fi} the expression

$$T_{fi} = -2^{7/2-i\eta}(i\eta)\alpha^{3/2}e^{\gamma\pi/2}\Gamma(1-i\gamma)\int_0^\infty ds\, s^{-i\eta-1}\int_0^1 dx F(s,x) \ , \tag{34}$$

where

$$F(s,x) = x^{-1}[\alpha-x^{-1}(1-x)s]\left[\frac{\partial}{\partial\alpha^2}\right]^2\left[A^{-i\eta}B^{i\eta-1}\mu^{-i\eta}\nu^{i\eta-1}\left[1+\frac{1}{\nu}\right]^{-i\gamma}{}_2F_1\left[i\gamma;i\eta;1;\frac{\mu-\nu}{\mu(\nu+1)}\right]\right] . \tag{35}$$

The exchange scattering amplitude g_{fi} can then be calculated from the relation

$$g_{fi} = -\frac{1}{2\pi}T_{fi} \ , \tag{36}$$

where T_{fi} is computed numerically using Gaussian quadratures after performing the parametric differentiation twice with respect to α^2.

The integration over s in (34) with an arbitrary small value of ϵ is well defined analytically in principle, but in practice it is hardly possible to evaluate it numerically. To make the integration numerically tractable for small s,

we have adopted the method of Onaga, Tsuji,and Narumi [4]. We rewrite Eq. (36) as

$$g_{fi}=c\int_0^\infty ds\, s^{-i\eta-1}J(s)\ , \tag{37}$$

where

$$J(s)=\int_0^1 dx F(s,x) \tag{38}$$

and

$$c=\frac{i\eta}{\pi}2^{5/2-i\eta}\alpha^{3/2}e^{\gamma\pi/2}\Gamma(1-i\gamma)\ .$$

In order to avoid the numerical difficulty stemming from the integrand in (37) for small values of s, we have put Eq. (37) into the following form by adding to the amplitude and then subtracting from it the same term:

$$g_{fi}=c\left[J(0)\int_0^1 ds\, s^{-i\eta-1}+\int_0^1 ds\, s^{-i\eta-1}(J(s)-J(0))+\int_1^\infty ds\, s^{-i\eta-1}J(s)\right]\ . \tag{39}$$

B. Evaluation of TDCS's

For the case where the incident beam and hydrogenic target are unpolarized and no attempt is made to distinguish between the final spin states, the TDCS's for the $H(e,2e)H^+$ process is given by

$$\frac{d^3\sigma}{d\hat{\mathbf{k}}_1 d\hat{\mathbf{k}}_2 dE_2}=\frac{k_1k_2}{k}[\tfrac{1}{4}|f+g|^2+\tfrac{3}{4}|f-g|^2]\ , \tag{40}$$

where f and g represent, respectively, the direct and exchange scattering amplitudes. In Eq. (40), $d\hat{\mathbf{k}}_1$ and $d\hat{\mathbf{k}}_2$ denote, respectively, the elements of solid angles for the scattered and ejected electrons and dE_2 represents the energy interval of the ejected electron. In the present calculation, we have adopted for g the expression (39) of Sec. II A, whereas for f we have used the two-dimensional expression for the Glauber amplitude obtained by Roy, Das, and Sil [9].

The GA does not take into account the correlation between the two emitting electrons in the final state. This correlation manifests itself by a conspicuous PCI effect. The salient feature of the PCI effect is that the electron-electron interaction allows for exchange of angular momentum and energy between the two continuum electrons during their travel from the reaction zone to the detectors. Consequently, the emitting electrons undergo both trajectory deflections and energy shifts. These deviations have been calculated recently within the framework of classical mechanics [10],

$$\theta_i(0)=\theta_i-\sin(\chi)\int_0^\infty dt\, r_1 r_1 r_{12}^{-3}\int_t^\infty dt'[r_i(t')]^{-2}\ , \quad i=1,2\ , \tag{41}$$

$$E_1(0)=E_1+\frac{1}{r_1}\bigg|_{t=0}-\int_0^\infty dt\,\dot{r}_1 r_{12}^{-3}(r_1-r_2\cos\chi)\ , \tag{42}$$

$$E_2(0)=E_2-\int_0^\infty dt\,\dot{r}_2 r_{12}^{-3}(r_2-r_1\cos\chi)\ , \tag{43}$$

where $\chi=\theta_1+\theta_2$. $\theta_i(0)$ and $E_i(0)$ are the respective scattering angles and energies at the boundary of the reaction volume. The reaction volume was determined empirically by Klar *et al* [10]. It depends on two arbitrary parameters r_{01} and r_{02}, which represent the initial positions of the two emitting electrons. Klar *et al.* arrived at the values of the aforesaid parameters after a systematic search for good values of these parameters, which depend only on the incident energy, but not on the energy of the ejected electron and the angle of scattering. We have adopted exactly the same values of r_{01} and r_{02} as those in the calculation of Klar *et al.* The values of r_{01} and r_{02} for different incident energies have been given in Sec. III. The initial values for $\theta_i(0)$ and $E_i(0)$ are, however, determined numerically from Eqs. (41)–(43). In the present case, we approximate the integrals (41)–(43) using straight-line trajectories obtained from the equations

$$E_1=\tfrac{1}{2}\dot{r}_1^2$$

and

$$E_2=\tfrac{1}{2}\dot{r}_2^2-\frac{1}{r_2}\ ,$$

with initial values $r_1(0)=r_{01}$ and $r_2(0)=r_{02}$.

This classical treatment of the PCI effect may then be incorporated in the Glauber approximation including exchange correction (GA-EC-PCI). The quantities $\theta_i(0)$ and $E_i(0)$ were taken from our Glauber-exchange calculation, and Eqs. (41)–(43) were used to incorporate a classical PCI effect to obtain E_i and θ_i, which we compare with experiment.

III. NUMERICAL RESULTS AND DISCUSSION

TDCS's for the $H(e,2e)H^+$ process have been measured by Ehrhardt *et al.* [11] in a coplanar geometry; i.e., the three vectors $\mathbf{k}$, $\mathbf{k}_1$, and $\mathbf{k}_2$ are in a plane. They decrease strongly with increasing momentum transfer. So

TABLE I. Magnitude of binary maxima (in a.u.) for electron-impact ionization of atomic hydrogen.

E (eV)	E_2 (eV)	θ_1 (deg)	GA[a]	GA-EC[b]
150	3	4	11.83	11.58
		10	3.17	3.01
		16	0.87	0.77
	5	4	8.53	8.30
		10	3.08	2.91
		16	1.09	0.96
	10	4	3.69	3.53
		10	2.14	2.00
		16	1.26	1.10
250	5	3	10.85	10.74
		8	3.41	3.31

[a]Present Glauber approximation.
[b]Present exchange-corrected Glauber approximation.

attention was paid to the so-called asymmetric kinematics, i.e., to small scattering angles θ_1, and $E_2 \ll E_1$. In the present work, we have calculated TDCS's at incident enrgies of 150 and 250 eV in the case of asymmetric kinematics and compared our results with the absolute measurements of Ehrhardt *et al.* At $E=150$ eV we have studied the distribution of the ejected electrons for $E_2=3$, 5, and 10 eV and $\theta_1=4°$, 10°, and 16°, whereas at $E=250$ eV we have examined TDCS's for $E_2=5$eV and $\theta_1=3°$ and 8°. In order to obtain TDCS's we have adopt-

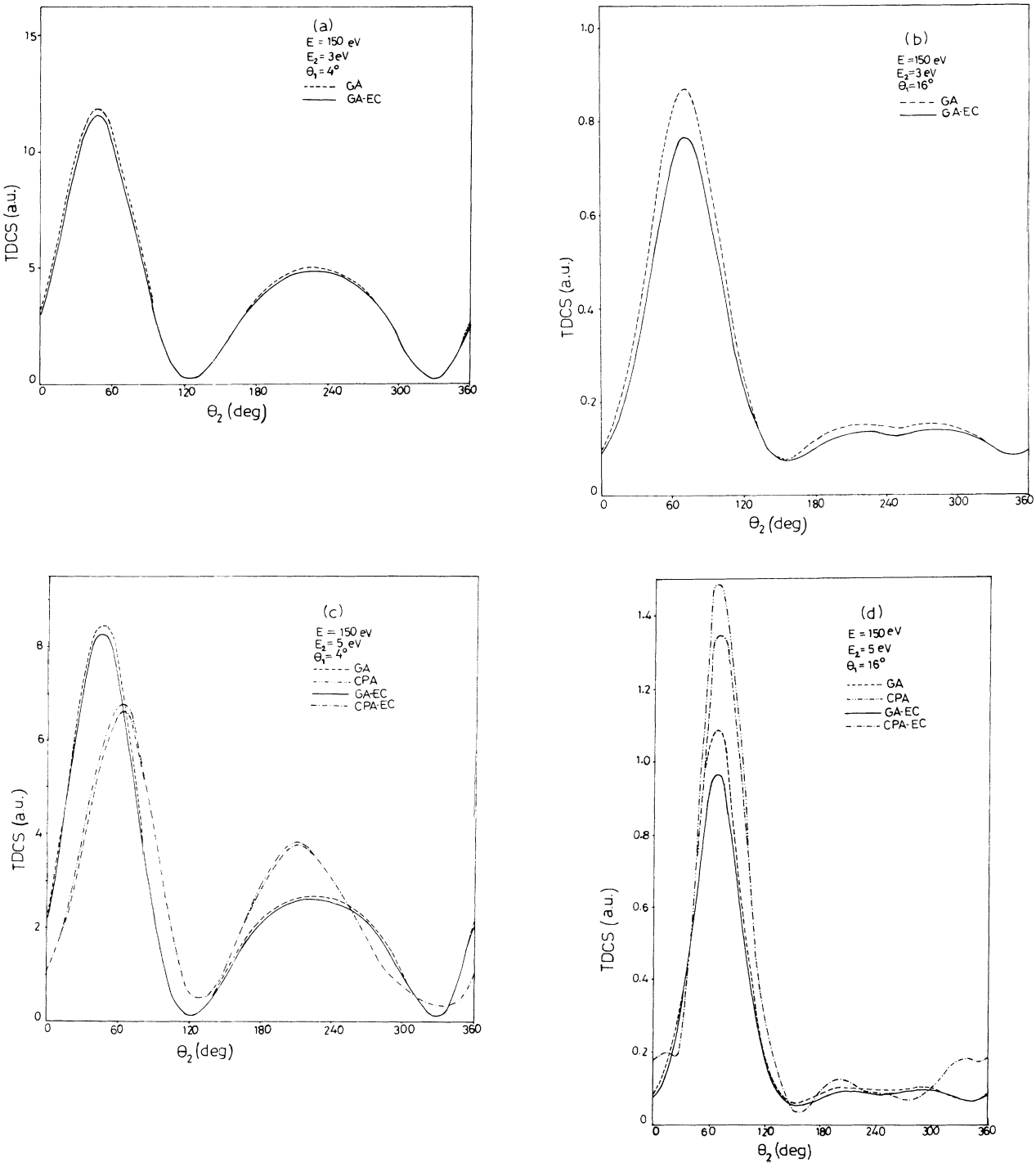

FIG. 1. TDCS vs the angle of ejection, θ_2, for the $H(e,2e)H^+$ reaction at an incident energy of 150 eV and energy of ejection, 3 eV, (a) $\theta_1=4°$ and (b) $\theta_1=16°$; energy of ejection, 5 eV, (c) $\theta_1=4°$ and (d) $\theta_1=16°$; and energy of ejection, 10 eV, (e) $\theta_1=4°$ and (f) $\theta_1=16°$. Curves: Glauber cross sections including exchange (solid curve), Glauber cross sections omitting exchange (dashed curve), coupled-pseudostate cross sections including exchange (dot-dashed curve), and coupled-pseudostate cross sections omitting exchange (double-dot-dashed curve).

ed the numerical procedure of Ref. [9] to calculate the direct amplitude, whereas the exchange amplitude given by (39) is evaluated using Gauss-Legendre quadratures for performing the x integration of Eq. (38) and Gauss-Laguerre quadratures for s integrals occurring in Eq. (39). Combining the exchange amplitude with the direct one by means of Eq. (40), we obtain the exchange-corrected Glauber cross sections.

At asymmetric kinematics, TDCS's obtained in the GA for the direct process are cylindrically symmetric around the momentum-transfer direction **q**. These theoretical cross sections show local maxima in the direction of the momentum-transfer vector **q** (binary peak) and $-\mathbf{q}$ (recoil peak). The binary peak is more pronounced than the recoil peak. Table I presents the magnitude of binary peaks obtained in the GA and the exchange-corrected Glauber approximation (GA-EC). Although the GA and the GA-EC predictions for the binary-peak positions are almost the same (not differing by more than 1°), the magnitudes of the binary peaks obtained in these methods differ. The GA-EC peak values are seen to be below the corresponding value of the GA peaks in all the cases considered in this work. Furthermore, we note that for fixed scattering angles the effect of exchange increases with increasing ejection energies, while the effect decreases with decreasing scattering angles for a fixed energy of ejection. More specifically, we note that at the fixed incident energy of 150 eV and fixed scattering angle of 4°, the TDCS decreases by 2% for $E_2=3$ eV, whereas it decreases by 4% when E_2 is increased to an energy of 10 eV. On the other hand, we find that for the same fixed incident energy of 150 eV and fixed ejection energy of 3 eV, the TDCS decreases by about 12% at $\theta_1=16°$ as against 2% at $\theta_1=4°$. The exchange effect is seen to be less pronounced at higher incident energies.

Figure 1 shows our GA and GA-EC results for the distribution of ejected electrons at the incident energy $E=150$ eV, ejection energy $E_2=3$, 5, and 10 eV, and scattering angles 4° and 16°. In that figure we illustrate the importance of exchange. As expected, the exchange effect is seen to be relatively more important with decreasing incident energy, increasing scattering angle, and increasing ejection energy. In Figs. 1(c) and 1(d), we have also displayed the results obtained in the coupled-pseudostate approximation (CPA) [15] with and without exchange. It should be noted that although the exchange in the CPA is considered through the proper antisymmetrization of the wave function, the exchange term in the coupled integro-differential equations has been neglected in the actual calculation. We note that our cross sections are in qualitative agreement with the corresponding results of CPA calculations. The cross sections are affected mainly in the vicinity of the binary peak and most consipicuously in the case where $E_2=10$ eV and $\theta_1=16°$.

Figure 2 displays the present TDCS's obtained in the GA and GA-EC at the higher incident energy $E=250$ eV, ejection energy $E_2=5$ eV, and scattering angles $\theta_1=3°$ and 8°. The exchange effect is seen to be almost unimportant. Its contribution to the cross section does not exceed 2% and 4% at any angle in Figs. 2(a) and 2(b), respectively.

Figures 3 and 4 show a comparison of the present GA-EC and GA-EC-PCI calculations and the measured TDCS's of Ehrhardt *et al.* [11]. The error bars on the measured data indicate the quoted normalization error of 15%. Also shown in the figures are the CPA results of Curran and Walters [15], the unitarized eikonal Born

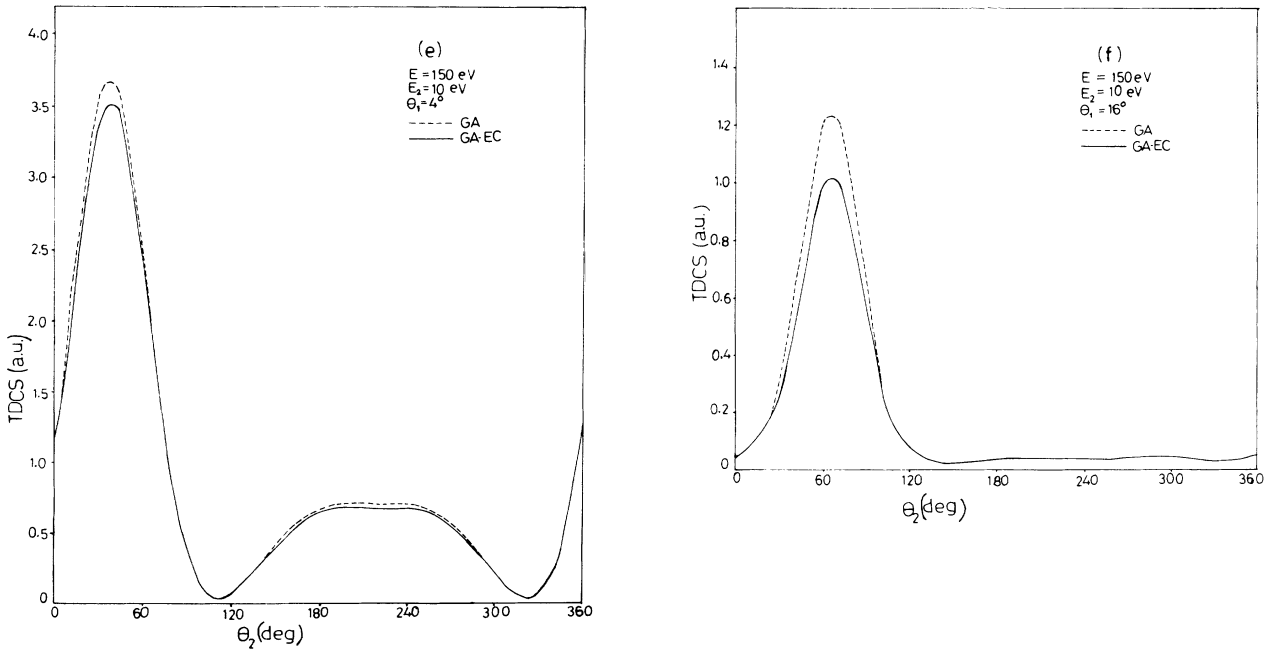

FIG. 1. (*Continued*).

series (UEBS) [16] cross sections of Joachain *et al.*, and the eikonal Born series results of Byron, Joachain, and Piraux [17]. The UEBS method consists in amalgamating the second Born and the Wallace approximation. Whereas the CPA takes care of exchange through the antisymmetrization of the final-state wave function, UEBS cross sections take into account exchange effects via the Ochkur-exchange amplitude. The EBS method adds the Glauber approximation to the third Born term to the first and second terms of the Born series. Exchange is included in the EBS calculation of Byron, Joachain, and Piraux through the Ochkur approximation. We see from Figs. 3 and 4 that the *ab initio* calculations, namely, the EBS, UEBS, CPA, and GA-EC, yield cross sections which have nearly similar features. However, the magnitudes of the cross sections obtained in these methods differ. At $E=250$ eV, the TDCS's predicted by the CPA and EBS are within the experimental error bars for both scattering angles $\theta_1=3°$ and 8°. On the other hand, the present GA-EC nearly reproduces the experimental data at $\theta_1=8°$. At $\theta_1=3°$ it is in reasonably good agreement with experiment, but underestimates the experimental findings in the recoil-peak region. At the smaller incident energy $E=150$ eV, the agreement between the CPA and experiment is not so good as before. At $\theta_1=16°$ the CPA cross sections are too large in the neighborhood of the binary peak. At the scattering angles of 4° and 10°, the UEBS curves lie below the experimental data in the vicinities of the recoil and binary peaks, respectively. In the remaining regions, the UEBS cross sections show quite good agreement with the measured values. The GA-EC cross sections are in reasonably good agreement with experiment at $\theta_1=16°$. This agreement decreases at lower scattering angles.

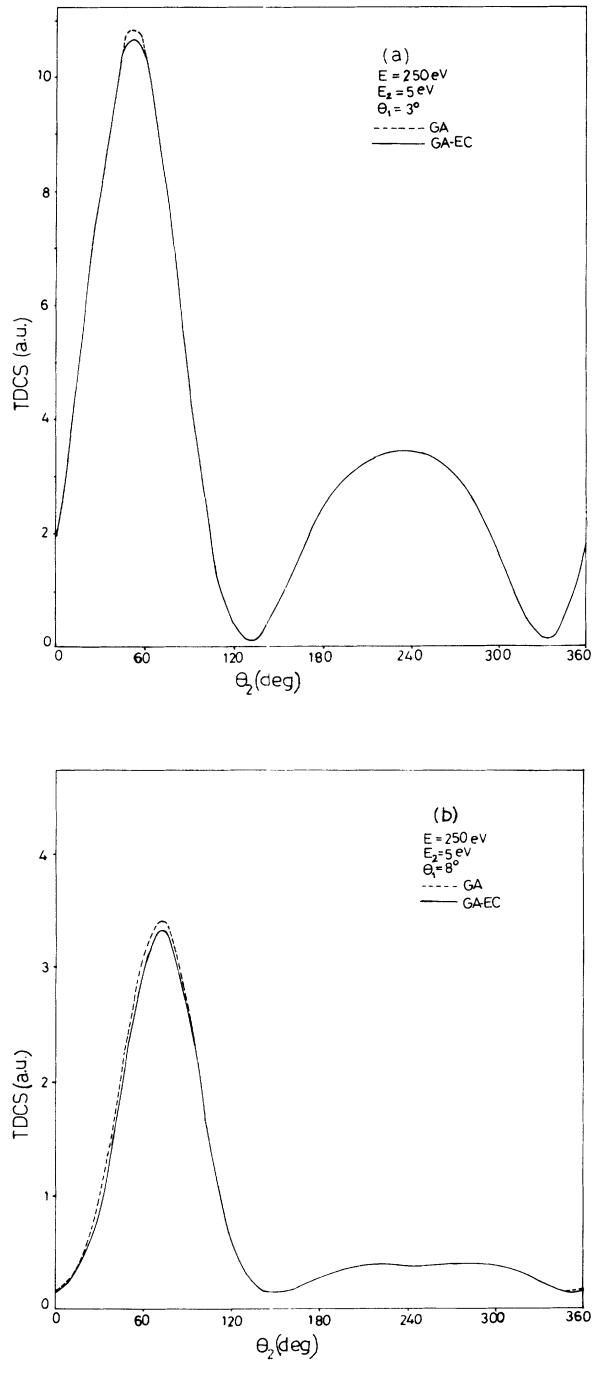

FIG. 2. Coplanar TDCS vs the angle of ejection, θ_2, for the $H(e,2e)H^+$ reaction at an incident energy of 250 eV, energy of ejection, 5 eV, and angle of scattering (a) $\theta_1=3°$ and (b) $\theta_1=8°$. Curves: Glauber cross sections including exchange (solid curve) and Glauber cross sections omitting exchange (dashed curve).

The present GA-EC-PCI calculation depends on two arbitrary parameters r_{01} and r_{02}. At the incident energy of 250 eV, the values chosen for r_{01} and r_{02} were, respectively, 3.1 and 0.4, whereas at $E=150$ eV these values were 2.4 and 0.4. We find that the inclusion of post-collision interaction improves the present GA-EC results considerably.

IV. CONCLUSIONS

We have presented a method of obtaining the exchange scattering amplitude for electron-impact ionization of atomic hydrogen. This method reduces the exchange scattering amplitude to a simple two-dimensional integral, which can be computed numerically with convenience.

We have calculated coplanar TDCS's for the $H(e,2e)H^+$ process at incident energies of 150 and 250 eV for a variety of ejected electron energies and scattering angles in the case of asymmetric geometry, i.e., $E_2 \ll E_1$ and θ_1 is small. The calculation is performed by combining the present eikonal amplitude with our previous Glauber amplitude. The effect of post-collision interaction is also incorporated in the present calculation. We find that exchange is relatively more important with decreasing incident energy, increasing scattering angle, and increasing ejection energy. These findings are consistent with those of the coupled-pseudostate work of Curran and Walters [15]. Exchange is found to cause a decrease in TDCS cross sections in all the cases studied in this work. It is found to be most prominent in the vicinity of the binary peaks. Furthermore, we note that the TDCS's obtained in the present PCI-modified exchange-corrected

Glauber approximation are in reasonably good agreement with experiment.

ACKNOWLEDGMENTS

This work is supported in part by the Institute for Theoretical Atomic and Molecular Physics, Cambridge. The authors are grateful to Professor N. C. Sil of Indian Association for the Cultivation of Science, Calcutta, for many valuable discussions.

APPENDIX

We consider in this appendix the integral

$$I=\oint_\Gamma dt\, t^{-1+i\alpha}(t-1)^{-i\alpha}(t+\mu)^{-i\eta}(t+\nu)^{i\eta-1}\ , \qquad \text{(A1)}$$

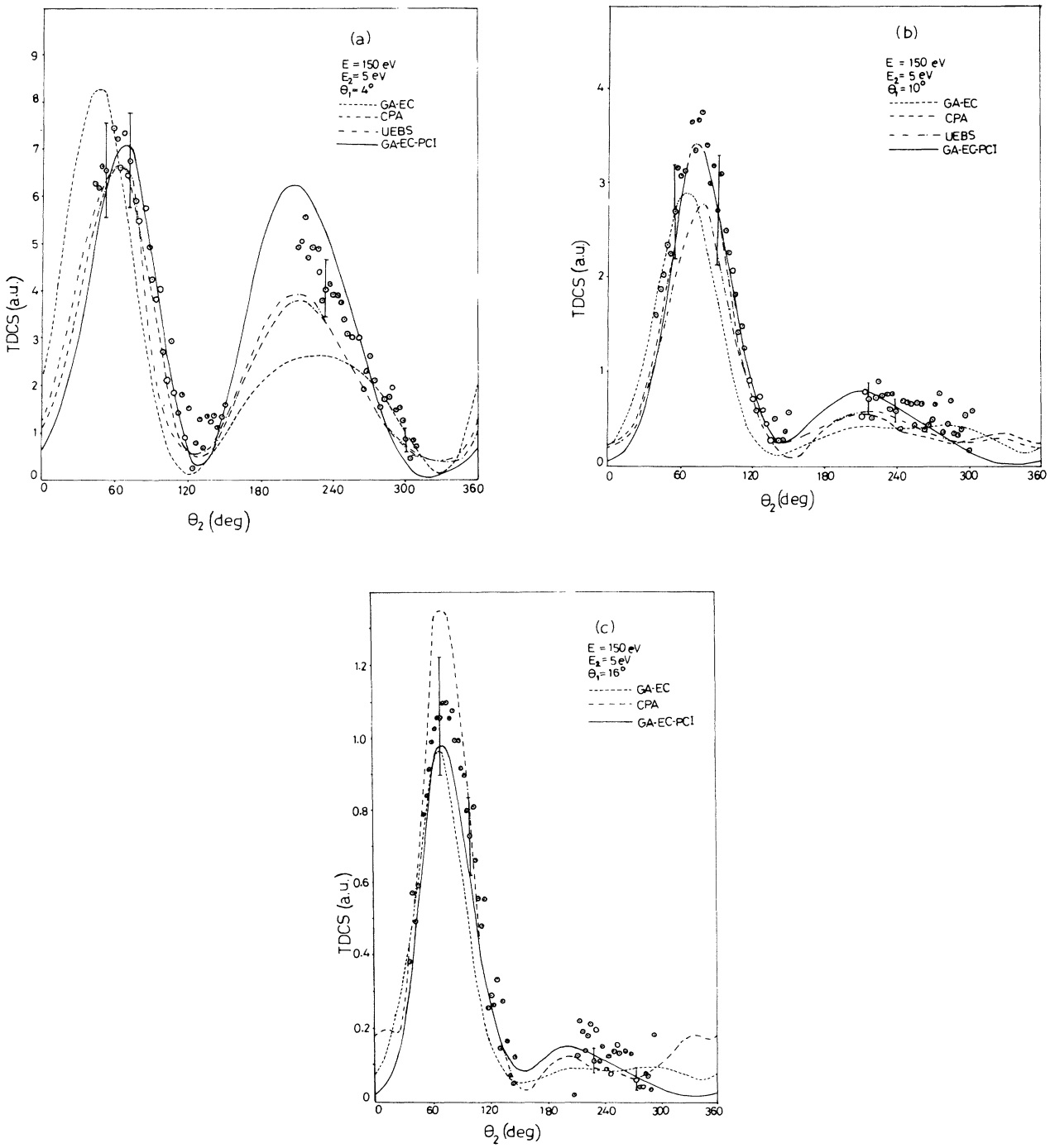

FIG. 3. Coplanar TDCS vs the angle of ejection for the $H(e,2e)H^+$ reaction at an incident energy of 150 eV, energy of ejection, 5 eV, and angle of scattering, (a) $\theta_1=4°$, (b) $\theta_1=10°$, and (c) $\theta_1=16°$. Curves: Glauber cross sections including PCI and exchange (solid curve), Glauber cross sections including exchange (dashed curve), coupled-pseudostate cross sections including exchange (dot-dashed curve), and UEBS approximation including exchange of Joachain *et al.* [16] (double-dot-dashed curve). Open circles are the results of the absolute measurements of Klar *et al* [10].

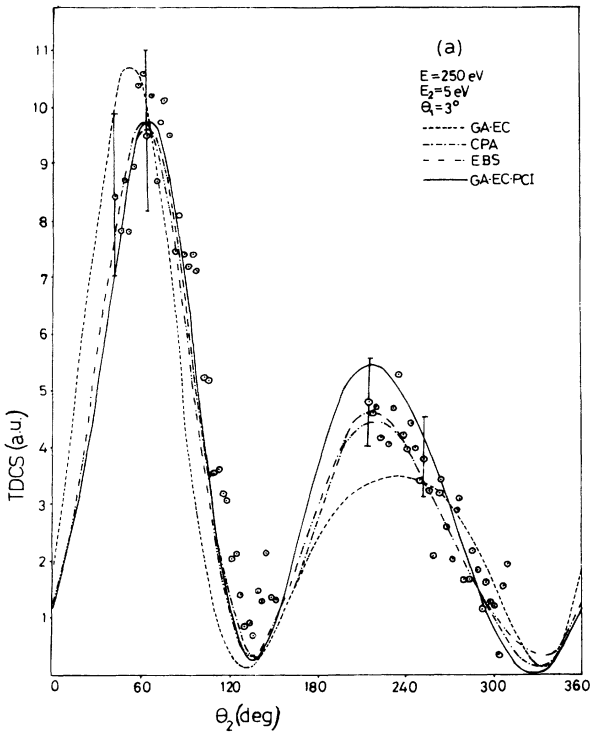

FIG. 4. Coplanar TDCS vs the angle of ejection for the $H(e,2e)H^+$ reaction at an incident energy of 250 eV, energy of ejection, 5 eV, and angle of scattering, (a) $\theta_1=3°$ and (b) $\theta_1=8°$. Curves: Glauber cross sections including PCI and exchange (solid curve), Glauber cross sections including exchange (dashed curve), coupled-pseudostate approximation including exchange (dot-dashed curve), and EBS approximation including exchange of Byron, Joachain, and Piraux [17] (double-dot-dashed curve). Open circles are the results of absolute measurements of Klar *et al.* [10].

where Γ indicates a closed contour encircling each of the two points 0 and 1 once counterclockwise.

Assuming

$$|\mu|\ ,|\nu|>|t| \tag{A2}$$

and using the expansion

$$(\mu+t)^{-i\eta}(\nu+t)^{i\eta-1}=\mu^{-i\eta}\nu^{i\eta-1}\times\sum_{n,s}(-1)^n\frac{\mu^{-n}t^n}{n!}(i\eta)_n\times(-1)^s\frac{\nu^{-1}t^s}{s!}(1-i\eta)_s\ , \tag{A3}$$

Eq. (A1) can be written as

$$I=\sum_{n,s}\oint_\Gamma dt\ t^{n+s+i\alpha-1}(t-1)^{-i\alpha}\mu^{-i\eta}\nu^{i\eta-1}\times(-1)^{n+s}\frac{\mu^{-n}\nu^{-s}}{n!s!}(i\eta)_n(1-i\eta)_s\ , \tag{A4}$$

provided condition (A2) is satisfied for all values of t on the contour.

Next, we consider the integral representation of the $\mathcal{B}$ function

$$\mathcal{B}(x,y)=\frac{1}{2\sinh(\pi iy)}\oint_\Gamma dt\ t^{x-1}(t-1)^{y-1}\ ,\quad \mathrm{Re}\,x>0\ . \tag{A5}$$

Letting $x=r+1-i\eta$, where r is positive and $y=i\eta$, Eq. (A5) can be expressed as

$$\mathcal{B}(r+1-i\eta,i\eta)=\frac{1}{2\sinh(-\pi\eta)}\oint_\Gamma dt\ t^{r-i\eta}(t-1)^{i\eta-1}\ . \tag{A6}$$

Now remembering the relations

$$(a)_r=\frac{\Gamma(a+r)}{\Gamma(a)}\ \text{and}\ \mathcal{B}(x,y)=\frac{\Gamma(x)\Gamma(y)}{\Gamma(x+y)}\ ,$$

$\mathcal{B}(r+1-i\eta,i\eta)$ can be written as

$$\mathcal{B}(r+1-i\eta,i\eta)=\frac{(1-i\eta)_r\pi}{r!\sin(\pi i\eta)}\ . \tag{A7}$$

Using (A7) in (A6), we have

$$\oint_\Gamma dt\ t^{r-i\eta}(t-1)^{i\eta-1}=\frac{2i\pi(1-i\eta)_r}{r!}\ . \tag{A8}$$

Utilizing relation (A8), Eq. (A4) can be written as

$$I=2\pi i\mu^{-i\eta}\nu^{i\eta-1}\sum_{n,s}\left[\frac{(i\alpha)_{n+s}(i\eta)_n(1-i\eta)_s}{(1)_{n+s}n!s!}\left[-\frac{1}{\mu}\right]^n\times\left[-\frac{1}{\nu}\right]^s\right]\ . \tag{A9}$$

The double summation in (A9) can now be performed [18]. Equation (A9) then becomes

$$I=2\pi i\mu^{-i\eta}\nu^{i\eta-1}F_1\left[i\alpha,i\eta,1-i\eta,1,-\frac{1}{\mu},-\frac{1}{\nu}\right]. \quad \text{(A10)}$$

The hypergeometric function F_1 of two variables occurring in Eq. (A10) can be expressed in terms of the Gaussian hypergeometric function ${}_2F_1$ using the relation [19]

$$F_1(\alpha,\beta,\beta',\beta+\beta';x,y)=(1-y)^{-\alpha}{}_2F_1\left[\alpha,\beta;\beta+\beta',\frac{x-y}{1-y}\right]. \quad \text{(A11)}$$

Consequently, the ingegral I can be written as

$$I=2\pi i\mu^{-i\eta}\nu^{i\eta-1}\left[1+\frac{1}{\nu}\right]^{-i\alpha}{}_2F_1\left[i\alpha,i\eta;1;\frac{\mu-\nu}{\mu(\nu+1)}\right]. \quad \text{(A12)}$$

Although we obtain the result (A12) under the restriction (A2), it is valid at other regular points by analytic continuation.

[1] See, for example, C. J. Joachain and C. Quigg, Rev. Mod. Phys. **46**, 279 (1974); E. Gerjuoy and B. K. Thomas, Rep. Prog. Phys. **37**, 1345 (1974); F. T. Chan, M. Lieber, G. Foster, and W. Williamson, Jr., in *Advances in Electronics and Electron Physics,* edited by L. Marton and C. Marton (Academic, New York, 1979), Vol. 49, p. 133.

[2] F. W. Byron, Jr. and C. J. Joachain, Phys. Lett. **38A**, 185 (1972).

[3] G. Foster and W. Williamson, Jr., Phys. Rev. A **13**, 2023 (1976).

[4] T. Onaga, A. Tsuji, and H. Narumi, J. Phys. B **20**, 4851 (1987).

[5] V. Franco and A. M. Halpern, Phys. Rev. A **26**, 2482 (1982).

[6] T. T. Gien, Phys. Rev. A **26**, 658 (1982).

[7] T. Sekimura and H. Narumi, Prog. Theor. Phys. **63**, 1797 (1980).

[8] H. Ehrhardt, K. Jung, G. Knoth, and P. Schlemmer, Z. Phys. D **1**, 3 (1986).

[9] A. C. Roy, A. K. Das, and N. C. Sil, Phys. Rev. A **23**, 1662 (1981).

[10] H. Klar, A. C. Roy, P. Schlemmer, K. Jung, and H. Ehrhardt, J. Phys. B **20**, 821 (1987).

[11] H. Ehrhardt, G. Knoth, P. Schlemmer, and K. Jung, Phys. Lett. **110A**, 92 (1985); and private communication.

[12] See, for example, F. W. Byron, Jr. and C. J. Joachain, Phys. Rep. **179**, 211 (1989).

[13] A. Nordsieck, Phys. Rev. **93**, 785 (1954).

[14] I. S. Gradshteyn and I. M. Ryzik, *Table of Integrals, Series and Products* (Academic, New York, 1985), p. 950.

[15] E. P. Curran and H. R. J. Walters, J. Phys. B **20**, 337 (1987).

[16] C. J. Joachain, B. Piraux, R. M. Potvliege, F. Furtado, and F. W. Byron, Jr., Phys. Lett. **112A**, 138 (1985).

[17] F. W. Byron, Jr., C. J. Joachain, and B. Piraux, J. Phys. B **18**, 3203 (1985).

[18] *Higher Transcendental Functions,* edited by A. Erdelyi (McGraw-Hill, 1953), Vol. 1, p. 224.

[19] See Ref. [14], p. 1054.